



OPEN Divergent neurodegeneration associations with choroid plexus volume and degree of calcification in cognitively normal APOE ϵ 4 carriers and non-carriers

Ilker Ozsahin^{1,2}✉, Xiuyuan Wang¹, Liangdong Zhou¹, Ke Xi¹, Seyed Hani Hojjati¹, Emily Tanzi¹, Thomas Maloney¹, Edward K. Fung³, Jonathan P. Dyke³, Kewei Chen⁴, Silky Pahlajani¹, Laura Beth McIntire¹, Ana Paula Costa^{1,5}, William Jones Dartora¹, Qolamreza R. Razlighi¹, Lidia Glodzik¹, Yi Li¹, Gloria C. Chiang¹, Henry Rusinek⁶, Mony J. de Leon¹ & Tracy A. Butler¹✉

Choroid plexus (CP), best known for producing CSF, also regulate inflammation and clear metabolic waste to maintain brain homeostasis. CP dysfunction is implicated in Alzheimer's Disease (AD), with MRI studies showing CP enlargement in AD. The basis for CP enlargement is unknown. We hypothesized that calcium deposition within CP, which increases with aging and in certain neurodegenerative conditions, might underlie pathologic CP enlargement and be linked to neurodegeneration. In 166 cognitively normal participants, we used multimodal imaging to examine CP structure (MRI-measured overall volume, CT-measured calcium volume), PET-measured A β , age, and APOE genotype as predictors of neurodegeneration, indexed as hippocampal volume. CP enlargement was associated with reduced hippocampal volume, particularly in APOE4 carriers. CP calcium was not independently associated with hippocampal volume. However, a significant interaction revealed APOE4 genotype-specific associations between CP calcium and neurodegeneration, with APOE4 carriers showing greater hippocampal volumes in association with greater CP calcium—opposite to our hypothesis. Results suggest that a factor other than calcium drives pathologic CP enlargement associated with neurodegeneration, with this factor especially important in APOE4 carriers. Candidate factors include lipids and inflammatory cells, which are known to accumulate in CP and be regulated by APOE. Our findings highlight CP as a critical locus for studying AD pathogenesis and the mechanisms by which APOE4 promotes AD.

Keywords Choroid plexus, Calcification, Neurodegeneration, APOE, PiB PET

Abbreviations

AD	Alzheimer's disease
A β	Amyloid- β
CP	Choroid plexus
ϵ 4-	ϵ 4 negative
ϵ 4+	ϵ 4 positive
GMM	Gaussian mixture model
GE	General electric

¹Department of Radiology, Brain Health Imaging Institute, Weill Cornell Medicine, 407 East 61st Street, 2nd floor, New York, NY 10065, USA. ²Operational Research Center in Healthcare, Near East University, Near East Boulevard, Nicosia/TRNC, 99138 Mersin 10, Turkey. ³Department of Radiology, Weill Cornell Medicine, 525 East 68th Street, New York, NY 10065, USA. ⁴Banner Alzheimer Institute, Arizona State University, 901 E Willetta St, Phoenix, AZ 85006, USA. ⁵Department of Psychiatry, University of Pittsburgh, Pittsburgh, PA 15213, USA. ⁶Department of Radiology, New York University, 660 1st Avenue, New York, NY 10016, USA. ✉email: ilker.ozsahin@neu.edu.tr; tab2006@med.cornell.edu

HU	Hounsfield units
LV	Lateral ventricle
NACC	National Alzheimer's Coordinating Center
ROI	Regions of interest
TICV	Total intracranial volume

Background

Alzheimer's disease (AD) is a devastating disease associated with brain deposition of amyloid- β (A β) and tau, and irreversible neurodegeneration. A β deposition occurs early in the AD process, decades before cognitive decline¹. In late-onset AD, A β accumulation is due to failed clearance – not overproduction^{2,3}. The strongest genetic risk factor for AD, the ϵ 4 allele of the APOE gene^{4–6}, is known to impair the rate of A β clearance⁷. However, the mechanisms of clearance failure in AD and in association with the APOE4 allele remain uncertain. As detailed in several comprehensive reviews^{3,8–10}, A β is normally removed from the brain by three main mechanisms: (1) fluid clearance including the recently described glymphatic system, (2) transport or degradation at the endothelial blood-brain barrier, and (3) transport across the blood-CSF barrier, which is the choroid plexus (CP). Of these mechanisms, the role of CP in A β clearance has received less research attention and is the focus of this study.

Until recently, the main function of the CP was considered to be production of CSF through blood filtration. Now, the CP is understood to play a critical role in maintaining brain homeostasis by clearing toxins and metabolic waste including A β ^{11–19}. CP also regulates inflammation^{20–22} and have been shown to play a role in neurogenesis²³. All of these processes are critical to AD pathogenesis.

Because CP dysfunction may be an early event in the pathologic cascade leading to AD^{15,16}, in vivo identification of CP abnormalities using neuroimaging could potentially identify individuals at risk of AD before any involvement of brain parenchyma. This has motivated several recent studies measuring CP volume using MRI. Intriguingly, these studies have consistently demonstrated larger CP in patients with AD compared to cognitively normal controls^{24–26} and in association with the severity of cognitive impairment^{24,25,27}. CP enlargement is also associated with older age in subjects with and without AD^{24,25,27,28}. In one of the only longitudinal studies of CP structural change, CP enlargement with aging was found to be significantly greater in individuals who experienced cognitive decline compared to those who remained cognitively stable²⁴. Importantly, CP enlargement was also strongly associated with APOE4 status, with APOE4 homozygotes showing a threefold faster rate of CP enlargement compared to heterozygotes and non-carriers²⁴.

Pathologic CP enlargement contrasts with atrophy of virtually all brain parenchymal structures with aging and AD. The basis of pathologic CP enlargement in human neuroimaging studies of AD is uncertain. We recently showed that the volume of calcium within CP – measured using a multimodal Computed Tomography (CT) and MRI method – contributes to CP overall volume measured using MRI²⁰. In that study, the volume of CP calcium but not CP overall volume, was associated with PET-measured cortical inflammation in healthy subjects. CP calcification is well known to increase with normal aging^{29,30} and has been associated with neurodegeneration^{31,32}. Our prior finding²⁰ suggested that the volume of calcium deposited within CP might be a more accurate/sensitive biomarker of CP dysfunction than CP overall volume, at least with respect to the role of CP in regulation of inflammation. It is unknown whether this may also be the case with respect to the role of CP in clearing A β and preventing neurodegeneration.

The purpose of this study is therefore to assess, in a large cohort cognitively normal subjects characterized by APOE genotype, cross-sectional associations between multimodally-measured CP structure (MRI-measured overall CP volume and CT-measured CP calcium volume) within the lateral ventricles, PET-measured A β burden and neurodegeneration. We use MRI-measured hippocampal volume as a proxy for Alzheimer's disease-related neurodegeneration, consistent with multiple studies showing that hippocampal atrophy is a robust and well-validated biomarker of neurodegeneration in AD^{33,34}. We quantify the relative contribution of APOE genotype, CP calcium volume, CP overall volume and A β burden to hippocampal volume. The long-term objective of this line of research is to determine whether CP structural abnormalities, including CP calcification measurable using widely-available CT, can serve as a biomarker of AD risk that can guide future targeted AD prevention strategies.

Methods

Subjects and assessment

Subjects included all cognitively normal subjects who underwent PiB PET-CT and MRI between 2009 and 2022 as part of several studies of aging conducted at Weill Cornell Medicine and New York University. Subjects were recruited from the community via advertising. Each study had slightly different inclusion criteria, but all required subjects to be medically healthy apart from common condition such as hypertension or hypercholesterolemia, without significant psychiatric disease and free from alcohol or substance abuse. While some studies enrolled patients with a known or suspected diagnosis of MCI or AD, this re-analysis was limited to subjects with normal cognition (defined below.) All studies were approved by the institutional review boards and have been performed in accordance with the Declaration of Helsinki. All subjects formally consented to participate in the study by completing and signing the required written consent forms.

Subjects underwent detailed assessment using the National Alzheimer's Coordinating Center (NACC) assessment battery³⁵ including the Clinical Dementia Rating (CDR) scale administered by a specialist physician. Assessment typically occurred within 6 months of neuroimaging. Subjects included in this analysis had CDR = 0, indicating no meaningful cognitive impairment.

Image acquisition

Image acquisition for this study took place over 15 years and two PET and three MRI scanners. Key acquisition parameters are summarized below with details provided in Supplementary Materials (Tables S1–S2). Potential confounding effects of different scanners and acquisition parameters were included as covariates in analysis.

PET acquisition and processing

PET scanning was performed at Weill Cornell Citigroup Biomedical Imaging Center on a General Electric (GE) Discovery LS PET/CT from 2009 to 2011 (G.E. Medical Systems, Milwaukee, WI) then on a Siemens Biograph PET/CT from 2011 to 2022 (Siemens, Knoxville, TN). Subjects were injected with ~550 MBq of locally synthesized ¹¹C-PiB. Scanning acquisition differed slightly between 2009 and 2022 but always included the 60–90 min period post-injection, which was analyzed for this study. PET voxel size ranged from 1.9 × 1.9 × 4.3 mm in the earliest scans to 1.0 × 1.0 × 2.0 mm more recently. Additional acquisition parameters are provided in Supplementary Materials (Table S1).

PET images were corrected for photon attenuation, scatter, and radioactive decay and processed using an in-house image processing pipeline validated and used previously³⁶. Briefly, processing consists of aligning dynamic PET frames to the first frame using rigid-body registration and averaging them to generate a static PET image, which is then co-registered to that subject's T1 MRI. Average PiB SUVR (reference = cerebellar gray) is then calculated within a Freesurfer-defined meta-region consisting of AD-vulnerable cortical regions (cingulate, precuneus, frontal, parietal and temporal lobes)³⁷.

CT acquisition

Before each PET acquisition, a CT scan was acquired for attenuation correction and neuroanatomic localization. CT acquisition parameters varied significantly over time due to hardware changes and increased focus on minimizing radiation exposure. On the GE scanner (2009–2011) tube current was 125 mA and current-exposure time product (exposure) was 1104 mAs. On the Siemens scanner (2011–present) automatic exposure control was instituted to reduce patient radiation exposure; tube currents ranged from 22 to 216 mA and exposure from 14 to 180 mAs. Visual review of CT scans showed decreased image quality (increased noise/graininess) for scans acquired after automatic exposure control was instituted. CT acquisition parameters (tube current) were therefore included as a covariate in statistical analysis.

MRI acquisition and processing

MRI was acquired on either a 1.5T GE Signa scanner or one of two 3T Siemens Prisma scanners. T1w and FLAIR images were used in analysis. Acquisition parameters, which varied over time and scanners, are provided in supplemental data. Notably, the earliest FLAIR images included as few as 32 3.3 mm slices; these were manually reviewed to ensure they included the full CP. Additional acquisition parameters are provided in Supplementary Materials (Table S2).

T1 MRI

T1 MRI was used for PET and CT co-registration and regions of interest (ROI) segmentation. T1 MRI images were processed with FreeSurfer version 7 (<http://surfer.nmr.mgh.harvard.edu>) recon-all pipeline with manual editing of the white and gray matter borders to correct any mis-segmentation. The following bilateral ROIs were used in analysis: hippocampi, cerebellar gray matter, a cortical meta-region consisting of AD-vulnerable regions³⁷, lateral ventricle and CP. The hippocampal ROI was divided by total intracranial volume (TICV) calculated using SPM12 (<https://www.fil.ion.ucl.ac.uk/spm>) and used as an index of neurodegeneration. Cerebellar gray matter was used as the reference for PiB PET SUVR calculation. Lateral ventricle (all horns: frontal, temporal and occipital) and the CP within the ventricles were combined into a ventricle + CP ROI. This combined ventricle + CP ROI identified the region where CP could be located, and was used in the algorithms described below to accurately measure CP overall volume and CP calcium volume through co-registration to different image modalities (FLAIR MRI for CP overall volume; CT for CP calcium volume.) This was necessary because visual review of the CP segmentation based on T1 MRI showed significant inaccuracies and calcium is not visible on T1 MRI.

FLAIR MRI

Volume of CP within all horns (frontal, temporal, occipital) of bilateral lateral ventricles was measured by co-registering T2-FLAIR images to the T1w anatomical space used for FreeSurfer segmentation. The ventricle + CP ROI defined on T1 MRI (as described above) was eroded by one voxel to avoid partial volume effects. The FLAIR image in the eroded LV + CP mask was then denoised using a 3D Gaussian filter with sigma = 0.5 and fitted into a Gaussian mixture model (GMM) with three components. Voxels that belonged to the cluster with the highest average intensity value were selected as the final CP segmentation. This method was validated by comparing it to expert manual tracing using an independent dataset of 40 subjects, showing an average Dice similarity coefficient of 0.82, indicating high spatial overlap, reproducibility and accuracy³⁸.

CP calcium quantification

CP calcium was measured using a validated automated method described previously²⁰. Briefly, CT was co-registered to T1w MRI and CT voxels within the Freesurfer-defined LV + CP mask with Hounsfield units (HU) greater than 80 were used as seeds to segment contiguous areas of calcium with the ventricle. We previously showed that this method had intraclass correlation coefficient of 0.982 with expert visual tracing²⁰.

All segmentations were reviewed manually for accuracy. As noted above, CT images acquired after 2011, when automatic radiation exposure control was instituted on the Siemens PET-CT scanner, had noticeably reduced

quality, though our CP calcium segmentation algorithm remained accurate. For this reason, tube current was included as a covariate in statistical analyses. CP calcium volume was normalized by TICV.

APOE4 genotype determination

APOE4 status (presence or absence of an APOE4 allele) was determined using standard polymerase chain reaction procedures. Study subjects were classified as APOE4 carriers (APOE4+) if they had at least one APOE4 allele and classified as APOE4 non-carriers (APOE4-) otherwise.

Statistical analysis

Analyses were performed in R and SPSS.

Descriptive statistics

Continuous variables (age, hippocampal volume, CP calcium, CP overall volume, PiB SUVr) were checked for normality using Shapiro-Wilk test and summarized by mean/std or median/range for the full group, and separately in APOE4 carriers and non-carriers.

Group comparisons between APOE4 carriers and non-carriers

Comparisons of continuous variables between APOE4 carriers and non-carriers used t-test (for normally distributed variables) or Mann Whitney test (for non-normally distributed variables). Comparisons of categorical variables (sex, binarized presence vs. absence of CP calcium) between APOE4 carriers and non-carriers used chi-square test.

Correlations

We used Spearman correlation to assess pairwise associations between continuous variables in the full sample and separately in APOE4 carriers and non-carriers. Because all variables were expected to correlate with age, analyses were conducted both with and without adjusting for age (i.e., using partial Spearman correlations). To control for multiple comparisons, p-values were corrected using the false discovery rate (FDR) method.

Multiple linear regression

All regression assumptions (normality, linearity, homoscedasticity, absence of multicollinearity) were checked. We used a variance inflation factor (VIF) < 5 as the threshold for multicollinearity³⁹. Boxplots were used to identify potential outliers.

We used multiple linear regression with dependent variable = hippocampal volume (our index of neurodegeneration) and key predictors = APOE4 genotype, CP calcium, CP overall volume, cortical PiB SUVr, age and sex. We included the following potentially confounding neuroimage acquisition parameters: MRI field strength (3T versus 1.5T), days between MRI and PET-CT scanning and CT tube current, which varied significantly over time due to institution of automatic radiation exposure control in 2011, and which affects CT image quality/noise and thus CP calcium quantification. Because prior studies have implicated APOE4 status as highly relevant to AD risk⁴⁻⁶, and possibly to CP structural changes²⁴, we assessed potential interactions between APOE4 status and CP measures.

Results

Subjects

From a total of 206 PiB PET scans from cognitively normal subjects, 40 were excluded for the following reasons: 36 subjects lacked either T1 or FLAIR MRI within 1 year of PET, 2 had FLAIR scans that were not full-brain and did not include CP, 1 PET scan had abnormally low counts, 1 subject with hippocampal volume 2 std below mean was re-reviewed and re-classified as cognitively impaired (MOCA = 16). This left 166 subjects. 21 subjects (12.7%) were A β + based on PiB SUVr > 1.3 in cortical region confirmed by visual interpretation.

Demographics and other characteristics of subjects are presented in Table 1.

Group differences between APOE4 carriers and non-carriers

As shown in Table 1, APOE4 carriers and non-carriers did not differ in terms of demographics, CP overall volume, CP calcium, or any other measured variables. 9/63 (14.3%) of APOE4 carriers and 15/103 (14.6%) of APOE4 non-carriers. had no detectable CP calcium; these percentages did not differ significantly ($p = .99$). Results were unchanged when one APOE4+ subject with the largest CP volume was excluded from analysis.

Correlation results

All correlation results are presented in Supplementary Materials.

We examined pairwise Spearman correlations among all continuous variables: age, CP overall volume, CP calcium volume, PiB SUVr, and hippocampal volume in the full sample ($N = 166$), as well as in APOE4 carriers and non-carriers separately. In the unadjusted full-sample analysis, age was significantly associated with greater CP volume ($\rho = 0.403, p < .001$), higher PiB SUVr ($\rho = 0.526, p < .001$), and lower hippocampal volume ($\rho = -0.506, p < .001$). CP overall volume correlated positively with PiB SUVr ($\rho = 0.225, p = .004$) and negatively with hippocampal volume ($\rho = -0.374, p < .001$). CP calcium volume was significantly associated only with CP overall volume ($\rho = 0.327, p < .001$). These patterns were broadly similar when stratified by APOE4 status.

After controlling for age, most associations were attenuated. In the full group, only the correlations between CP overall volume and CP calcium volume ($\rho = 0.308, p < .001$), and between CP overall volume and hippocampal volume ($\rho = -0.216, p = .005$), remained significant. In the age-adjusted, APOE-stratified analyses, a genotype-dependent effect emerged: the correlation between CP overall volume and hippocampal volume was significant

	Total	APOE4+	APOE4-	Statistical test	<i>p</i>
Demographics					
Number of subjects	166 (100%)	63 (37.9%)	103 (62.1%)	n/a	n/a
Mean age (sd)	59.95 (12.85)	59.47 (11.98)	60.24 (13.40)	Mann–Whitney	0.58
Sex	F: 109 (65.7%) M: 57 (34.3%)	F: 44 (69.8%) M: 19 (30.2%)	F: 65 (63.1%) M: 38 (36.9%)	Chi square	0.38
Image acquisition					
PET scanner	GE: 71 (42.8%) Siemens: 95 (57.2%)	GE: 25 (39.7) Siemens: 38 (60.3%)	GE: 46 (44.7%) Siemens: 57 (35.3%)	Chi square	0.53
MRI field strength	1.5T: 121 (72.9%) 3T: 45 (27.1%)	1.5T: 51 (81.0%) 3T: 12 (19.0%)	1.5T: 70 (68.0%) 3T: 33 (32.0%)	Chi square	0.07
3T MRI location	NYU : 18 (40%) WCM : 27 (60%)	NYU : 4 (33.3%) WCM : 8 (66.7%)	NYU : 14 (42.4%) WCM : 19 (57.6%)	Chi square	0.18
Mean CT exposure in mAs (sd)	519.90 (507.81)	492.08 (501.57)	536.92 (513.27)	Mann–Whitney	0.82
Mean CT tube current in mA (sd)	119.16 (47.35)	125.49 (47.07)	115.29 (47.32)	Mann–Whitney	0.11
Mean days between MRI and PET (sd)	105.25 (96.43)	108.33 (95.80)	103.37 (97.23)	Mann–Whitney	0.53
Neuroimaging results					
Mean CP calcium volume relative to TICV * 1000 (sd)	0.21 (0.20)	0.19 (0.18)	0.23 (0.21)	Mann–Whitney	0.43
Mean CP overall volume relative to TICV * 1000 (sd)	1.41 (0.70)	1.46 (0.88)	1.38 (0.55)	Mann–Whitney	0.80
Mean Hippocampal volume relative to TICV * 1000 (sd)	5.67 (0.53)	5.67 (0.54)	5.67 (0.53)	T-test	0.98
Mean Cortical PiB SUVR (sd)	1.21 (0.24)	1.28 (0.31)	1.17 (0.18)	Mann–Whitney	0.22

Table 1. Participant characteristics and neuroimaging parameters.

Variable	Unstandardized β	<i>P</i> value
Age	-0.016	< 0.001
Sex	-0.226	0.005
APOE4 genotype	-0.175	0.106
CP calcium volume	-0.174	0.453
CP overall volume	-0.153	0.031
Cortical AB (11 C-PiB SUVR)	-0.194	0.236
CT tube current	0.002	0.097
MR Field strength (3T vs. 1.5T)	0.016	0.823
Days between MRI and PET scanning	0.000	0.650
Interaction between CP calcium and APOE4 genotype	0.001	0.047

Table 2. Multiple regression model ($R^2 = 0.345$, R^2 adjusted = 0.30, $p < .001$) predicting hippocampal volume in 165 cognitively normal subjects. Age, sex, CP overall volume, and the interaction between CP calcium volume and APOE4 genotype were significant predictors. All volumes are normalized to total intracranial volume. Genotype is binarized presence vs. absence of an APOE4 allele.

in APOE4 carriers ($\rho = -0.420$, $p < .001$), but not in non-carriers ($\rho = -0.081$, $p = .417$), and this difference was statistically significant ($p = .025$, two-tailed Fisher r -to- z test). This suggests that, independent of age, CP enlargement is associated with reduced hippocampal volume only in individuals carrying an APOE4 allele.

Multiple regression results

One subject with the largest CP overall volume (6.52 vs. median = 1.32), who was APOE4-positive, was identified as an outlier based on boxplot analysis and was excluded from analysis. As shown in Table 2, age, sex, CP overall volume, and the interaction between APOE4 status and CP calcium were found to be significant predictors of hippocampal volume. Women had larger hippocampi (normalized by TICV) than men. The interaction between APOE4 status and CP calcium was due to a significant difference in the relation between CP calcium and hippocampal volume in APOE4 carriers as compared to non-carriers, as shown in Fig. 1. No other interactions were significant.

To clarify the basis for this interaction, we performed multiple regression analysis for APOE4 carriers and non-carriers separately. We found that in APOE4 carriers, CP overall volume ($\beta = -0.255$, $t = -2.481$, $p = .016$), sex ($\beta = -0.338$, $t = -2.190$, $p = .033$), and at a trend level, CP calcium ($\beta = 0.639$, $t = 1.900$, $p = .063$), age ($\beta = -0.013$, $t = -1.862$, $p = .068$), and the CT tube current ($\beta = 0.003$, $t = 1.809$, $p = .076$) predicted hippocampal volume. In APOE4 non-carriers, only age ($\beta = -0.018$, $t = -4.471$, $p < .001$) predicted hippocampal volume. The inverse association of CP overall volume and hippocampal volume (greater CP volume associated with reduced hippocampal volume) only in APOE4 carriers in this analysis mirrors results from the correlation analysis.

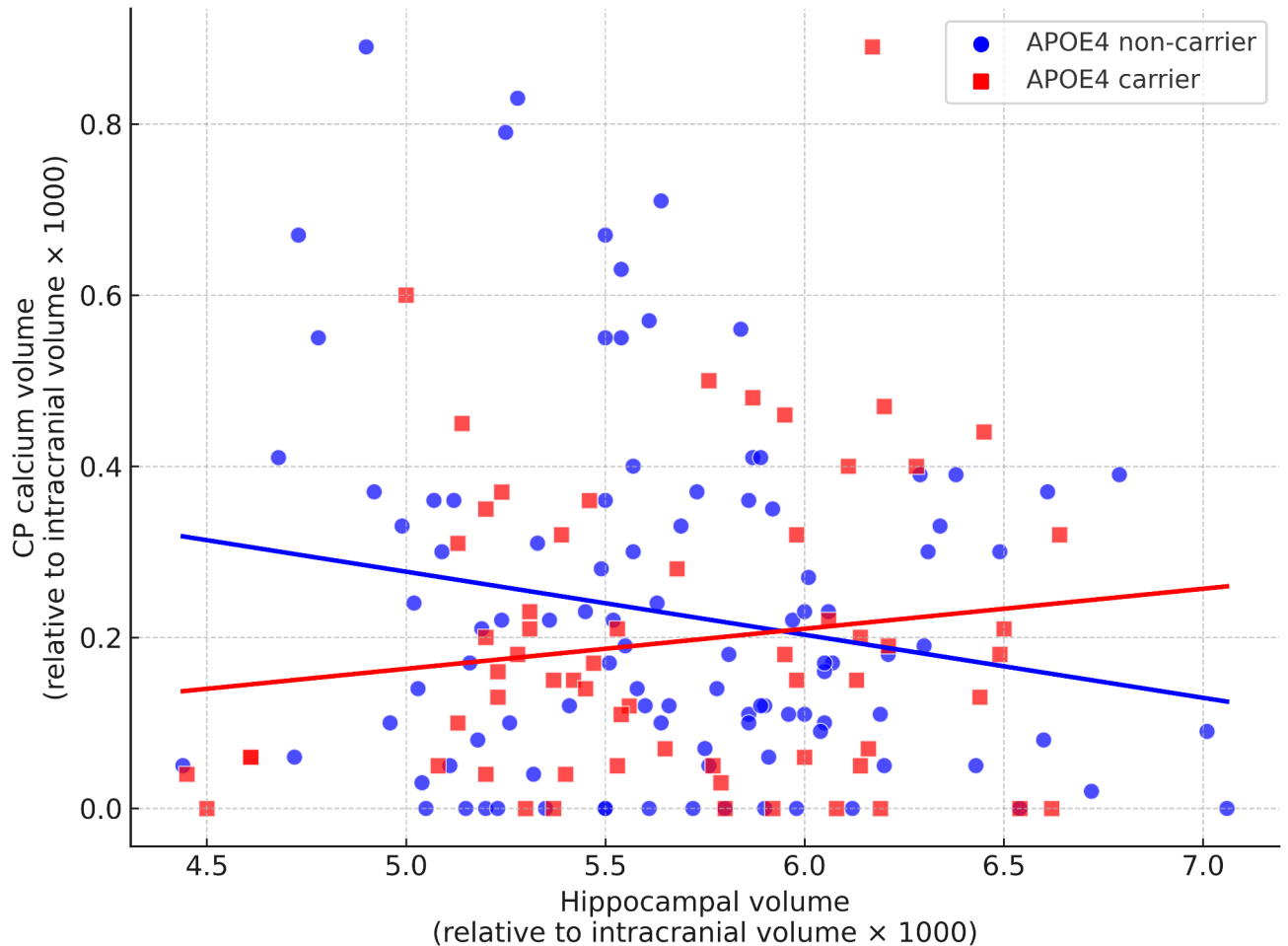


Fig. 1. Divergent association between choroid plexus calcium and hippocampal volume in APOE4 carriers vs. non-carriers. Scatter plot showing the relationship between CP calcium volume and hippocampal volume, both normalized by total intracranial volume, stratified by APOE4 status. The differing slopes illustrate the significant interaction between CP calcium and APOE4 status observed in the regression analysis, after adjusting for additional variables.

Discussion

This first neuroimaging study linking multimodally measured CP volume and calcification to AD neuroimage biomarkers contributes to the growing body of research linking CP structural abnormalities to neurodegeneration and AD pathogenesis, highlighting that the important role of CP in maintaining brain health and homeostasis extends far beyond its traditionally-recognized function of CSF production. We found, in 166 well-characterized, cognitively normal subjects, that MRI-measured CP enlargement was associated with reduced hippocampal volume – an index of neurodegeneration, with this association strongest in APOE4 carriers. This results adds to mounting evidence that CP enlargement is pathological^{24–28}. CP calcium was not independently associated with hippocampal volume. However, a significant interaction revealed APOE4 genotype-specific associations between CP calcium and neurodegeneration. As discussed below, we believe these findings offer important mechanistic insight into how choroid plexus structural alterations may interact with APOE4 genotype to influence vulnerability to neurodegeneration and drive key processes in AD pathogenesis.

The now well-established observation that CP enlargement signifies pathology, in contrast to the rest of the brain where pathology is marked by volume loss / atrophy, prompts the critical question: what is the basis of CP enlargement? To investigate this, we used multimodal neuroimaging to measure the volume of calcium deposited within CP. We used the CT scan acquired at the time of PET (for attenuation correction) and a validated CT-MRI segmentation method we developed²⁰ to quantify calcium, which cannot easily be quantified accurately using MRI^{40,41}. Based on clinical knowledge that CP calcification increases with normal aging and in certain forms of neurodegeneration^{29–32}, and our recent finding that cortical inflammation correlated closely with CP calcium volume (more so than CP overall volume)²⁰, we had hypothesized that the volume of calcium within CP might be a more accurate/sensitive biomarker of CP pathology than CP overall volume, and might therefore be more closely linked to neurodegeneration. This hypothesis was *not* confirmed. Even though the volume of calcium within CP correlated with overall CP volume (as expected, and as we showed previously²⁰), we found no evidence that the volume of calcium within CP was more specifically associated with neurodegeneration. In fact, we found

an unexpected trend towards the opposite in APOE4 carriers. As detailed below, we believe these intriguing dissociations in the correlation of CP calcium as compared to CP overall volume with hippocampal volume, and in APOE4 carriers versus non-carrier, provide novel insight into the role of CP in neurodegeneration, and how the APOE4 genotype promotes AD pathogenesis.

Greater MRI-measured CP volume is associated with reduced hippocampal volume – an index of neurodegeneration

Using simple correlation analysis (with or without controlling for age) as well multiple regression that accounted for additional relevant biological factors (age, sex, APOE4 status) and potential methodologic confounds such as neuroimage acquisition parameters, we found that larger MRI-measured CP overall volume was associated with lower hippocampal volume – an index of neurodegeneration. Larger CP overall volume was also associated with older age, though the association of CP overall volume and hippocampal volume was independent of age. These findings align with prior MRI studies of CP structure and confirm that increased CP volume is pathological^{24–28}.

The association between larger overall CP volume and reduced hippocampal volume appears to be driven by APOE4 carriers

When correlation and regression analyses were performed separately for APOE4 carriers and non-carriers, a significant inverse association between CP volume and hippocampal volume was observed only in APOE4 carriers. Although the interaction effect (genotype by overall CP volume) was not significant in the full group analysis, results indicate that the inverse relationship between CP overall volume and hippocampal volume may be more pronounced in APOE4 carriers. These findings are broadly consistent with a prior study demonstrating that APOE4 carrier status is associated with markedly accelerated choroid plexus enlargement over time, suggesting that the E4 allele may influence dynamic CP changes during aging²⁴.

Significant interaction between APOE4 genotype and CP calcium on hippocampal volume

Multiple regression analysis did identify a significant interaction between APOE4 genotype and CP calcium volume on hippocampal volume ($p = .047$). As illustrated in Fig. 1, in APOE4 carriers, there was a trend ($p = .063$) suggesting that higher CP calcium was associated with greater hippocampal volume. In contrast, APOE4-negative individuals showed an opposite pattern.

The pattern in APOE4 non-carriers is expected. Decades of clinical and research work, starting with pneumoencephalography in the early 1900s, has documented CP calcification in association with normal aging and in some forms of neurodegeneration^{29–32}. Based on this, we had hypothesized that CP calcium volume would be inversely associated with an index of neurodegeneration (hippocampal volume). However,

this hypothesis was not confirmed, and in APOE4-positive subjects, we found trend-level evidence for the opposite.

The association of neurodegeneration with greater CP overall volume but (in APOE4 carriers) lower CP calcium indicates that a substance/process other than calcium underlies pathologic CP enlargement, and this substance/process may be especially important in E4 carriers

The unexpected positive, trend-level association of greater CP calcium volume with greater hippocampal volume in APOE4 carriers, coupled with a strong, inverse association between CP overall volume and hippocampal volume, indicates that the deposition of substances other than calcium within CP and/or other structural CP alterations are responsible for the link between CP enlargement and neurodegeneration. Understanding what other than calcium could be causing pathologic CP enlargement, which we and one prior study²⁴ have shown to be most prominent in E4 carriers, has the potential to provide insight into the broader mechanisms by which the APOE4 allele promotes the AD pathogenetic process. Mechanisms proposed to underly the AD-promoting effect of the APOE4 allele include more severe blood-brain-barrier breakdown, greater inflammation, abnormal iron metabolism and lipid dyshomeostasis^{5–7}. Any of these mechanisms could be relevant to our results given that that inflammatory cells, iron and cholesterol are all known to accumulate in CP^{19,25,42}. Particularly intriguing is a recent human neuropathology demonstration of greater lipid deposition and associated complement-mediated inflammation in CP from E4 carriers with or without AD⁴³. That study also found that the amount of lipid deposited within CP correlated with the extent of A β and tau deposition⁴³. An in vitro study found that APOE4 is a less effective acceptor of cholesterol excreted from CP epithelial cells, causing cholesterol accumulation within CP in E4 cells⁴⁴. Our in vivo results, coupled with these neuropathological and mechanistic studies, implicate CP as a key locus for understanding how the APOE4 allele promotes the AD pathogenetic process.

Sex differences

Women had larger hippocampi (normalized by TICV) than men. This has been reported previously^{45,46}, though the magnitude of this effect in our small sample is somewhat surprising. The female sex hormone estrogen has important, beneficial effects on hippocampal structure^{47,48}, and decreased estrogen along with compensatory increased gonadotropins at menopause are considered a key explanation for increased rates of AD in women after menopause^{49,50}. It is a limitation of this study that we do not have information about subjects' menstrual or menopausal status in order to better interpret this finding. We controlled for sex in all analyses.

Lack of association of CP structure with A β deposition

We were not able to demonstrate an association between CP structure (neither overall nor calcium volume) and level of A β deposition. The association between CP overall volume and A β in our correlation analysis was caused by age, since both increase with age. Given that preclinical and neuropathological studies implicate CP failure in A β accumulation^{11,12,25,43}, with mounting evidence that CP dysfunction may be reflected in MRI-measurable

enlargement, it would be premature to give up on demonstrating an association between CP structure and A β deposition. A key limitation of our analysis is that we did not incorporate Bayes factors, which means we cannot support the absence of a relationship between CP structure A β ; rather, we can only conclude that we failed to reject the null hypothesis of no relationship⁵¹. Our negative findings may relate to limited sample size and our inclusion of only cognitively normal subjects with a small number of A β + subjects (21/166; 12.7%). It is also possible that CP structural alterations are more associated with tau than A β ^{52,53}. Future studies should assess CP structure in association with wider range in level of A β deposition, as well as in association with brain tau deposition.

Additional limitations

Because scans for this study were acquired over many years, there were changes in scanner hardware, which affected some measures. We used the CT acquired with PET-CT to measure CP calcium. Quantifying brain calcium is challenging using MRI, and CT is considered the gold standard for this. However, over recent years, in order to minimize unnecessary radiation exposure, the radiation dose of CT needed only for PET attenuation correction has been significantly reduced, and automated exposure control implemented. Addressing this limitation, we included CT parameters, as well as MRI parameters (3T vs. 1.5T) as covariates in analysis. In the near future, calcium sensitive MRI methods⁵⁴ may obviate the need for CT to measure brain calcification.

Another limitation of our study is the reliance on hippocampal volume as the sole measure of neurodegeneration. While MRI-measured hippocampal volume has been shown to correlate with neuropathological evidence of neuronal loss and AD pathology³⁴, it is not a direct marker of neurodegeneration. Instead, progressive hippocampal atrophy over time provides a more accurate reflection of the neurodegenerative process. The absence of longitudinal data in our study is therefore a significant limitation, as it prevents us from assessing changes in hippocampal volume, as well as meaningful change in cognition.

Conclusion

Our results demonstrate that MRI-measured CP enlargement is associated with neurodegeneration, indexed as lower hippocampal volume, in cognitively normal subjects, with this effect driven by APOE4 carriers. We also confirmed greater CP volume in association with older age. These findings add to the growing body of research indicating that CP enlargement is pathological^{24–28}, and emphasize that the important role of CP in maintaining brain health and homeostasis extends far beyond its traditionally-recognized function of CSF production.

With the goal of understanding the basis for pathologic CP enlargement, we used a validated, multimodal CT+MRI technique to measure the volume of calcium deposited within CP²⁰. We had thought CP calcium would be a more sensitive measure of CP pathology than overall CP volume, but this hypotheses was not confirmed. What we did find is a divergent association between CP calcium and hippocampal volume depending on APOE genotype. Specifically, we found a trend towards greater hippocampal volume with greater CP calcium volume in E4 carriers – the opposite of what we had hypothesized. This suggests that pathologic CP enlargement in association with neurodegeneration is due to substances and/or processes other than calcium, with these substances/processes especially relevant in E4 carriers.

Based on recent neuropathology study⁴³, a likely substrate for pathological, MRI-measurable CP enlargement that is more prominent in E4 carriers, may be lipids and inflammatory cells. This study demonstrated greater lipid and associated complement-mediated inflammation in the CP epithelia of E4 carriers, and in correlation with AD lesions⁴³. Additional work, including direct correlation between in vivo neuroimaging findings and ex vivo neuropathology would be needed to confirm this. Investigating APOE genotype-specific changes in CP structure can provide valuable insight into the broader mechanisms by which the APOE4 allele contributes to AD pathogenesis, which remain highly debated⁵⁶. The present neuroimaging findings in combination with available neuropathological studies⁴³ offer support for dysregulated inflammation and lipid metabolism as key to understanding of how AD progression may differ between APOE4-positive and APOE4–negative individuals^{56,55}, and highlight the CP as a key locus of these differences. Such insights are of considerable interest and therapeutic relevance, particularly given the recent availability of monoclonal antibody therapies for AD, which have demonstrated an unfavorable risk/benefit profile in APOE4 homozygotes⁵⁶.

Data availability

The datasets used and/or analyzed during the current study available from the corresponding author on reasonable request.

Received: 2 October 2024; Accepted: 4 April 2025

Published online: 14 April 2025

References

1. Jack, C. R. et al. Tracking pathophysiological processes in Alzheimer's disease: an updated hypothetical model of dynamic biomarkers. *Lancet Neurol.* **12** (2), 207–216 (2013).
2. Mawuenyega, K. G. et al. Decreased clearance of CNS β -amyloid in Alzheimer's disease. *Science* **330** (6012), 1774–1774 (2010).
3. Tarasoff-Conway, J. M. et al. Clearance systems in the brain—implications for alzheimer disease. *Nat. Reviews Neurol.* **11** (8), 457–470 (2015).
4. Farrer, L. A. et al. Effects of age, sex, and ethnicity on the association between Apolipoprotein E genotype and alzheimer disease: a meta-analysis. *Jama* **278** (16), 1349–1356 (1997).
5. Jiang, S. et al. A systems view of the differences between APOE E4 carriers and non-carriers in Alzheimer's disease. *Front. Aging Neurosci.* **8**, 171 (2016).
6. Yamazaki, Y., Zhao, N., Caulfield, T. R., Liu, C.-C. & Bu, G. Apolipoprotein E and alzheimer disease: pathobiology and targeting strategies. *Nat. Reviews Neurol.* **15** (9), 501–518 (2019).

7. Castellano, J. M. et al. Human ApoE isoforms differentially regulate brain amyloid- β peptide clearance. *Sci. Transl. Med.* **3** (89), 89ra57–89ra57 (2011).
8. Abbott, N. J., Pizzo, M. E., Preston, J. E., Janigro, D. & Thorne, R. G. The role of brain barriers in fluid movement in the CNS: is there a 'glymphatic' system? *Acta Neuropathol.* **135**, 387–407 (2018).
9. Mestre, H., Mori, Y. & Nedergaard, M. The brain's glymphatic system: current controversies. *Trends Neurosci.* **43** (7), 458–466 (2020).
10. Hladky, S. B. & Barrand, M. A. Elimination of substances from the brain parenchyma: efflux via perivascular pathways and via the blood–brain barrier. *Fluids Barriers CNS.* **15** (1), 1–73 (2018).
11. González-Marrero, I. et al. Choroid plexus dysfunction impairs beta-amyloid clearance in a triple Transgenic mouse model of Alzheimer's disease. *Front. Cell. Neurosci.* **9**, 17 (2015).
12. Alvira-Botero, X. & Carro, E. M. Clearance of amyloid-beta peptide across the choroid plexus in Alzheimer's disease. *Curr. Aging Sci.* **3** (3), 219–229 (2010).
13. Wolburg, H. & Paulus, W. Choroid plexus: biology and pathology. *Acta Neuropathol.* **119** (1), 75–88 (2010).
14. Johanson, C. et al. Homeostatic capabilities of the choroid plexus epithelium in Alzheimer's disease. *Cerebrospinal Fluid Res.* **1**, 1–16 (2004).
15. Serot, J.-M., Béné, M.-C. & Faure, G. C. Choroid plexus, aging of the brain, and Alzheimer's disease. *Front. Bioscience-Landmark.* **8** (6), 515–521 (2003).
16. Gião, T., Teixeira, T., Almeida, M. R. & Cardoso, I. Choroid plexus in Alzheimer's disease—the current state of knowledge. *Biomedicine* **10** (2), 224 (2022).
17. Krzyzanowska, A. et al. Expression of regulatory proteins in choroid plexus changes in early stages of alzheimer disease. *J. Neuropathology Experimental Neurol.* **74** (4), 359–369 (2015).
18. Perez-Gracia, E., Blanco, R., Carmona, M., Carro, E. & Ferrer, I. Oxidative stress damage and oxidative stress responses in the choroid plexus in Alzheimer's disease. *Acta Neuropathol.* **118**, 497–504 (2009).
19. Stopa, E. G. et al. Comparative transcriptomics of choroid plexus in Alzheimer's disease, frontotemporal dementia and Huntington's disease: implications for CSF homeostasis. *Fluids Barriers CNS.* **15** (1), 1–10 (2018).
20. Butler, T. et al. Choroid plexus calcification correlates with cortical microglial activation in humans: a multimodal PET, CT, MRI study. *Am. J. Neuroradiol.* (2023).
21. Fleischer, V. et al. Translational value of choroid plexus imaging for tracking neuroinflammation in mice and humans. *Proc. Natl. Acad. Sci. U S A.* **118** (36), e2025000118 (2021).
22. Kunis, G. et al. IFN- γ -dependent activation of the brain's choroid plexus for CNS immune surveillance and repair. *Brain* **136** (11), 3427–3440 (2013).
23. Johanson, C., Stopa, E., Baird, A. & Sharma, H. Traumatic brain injury and recovery mechanisms: peptide modulation of periventricular neurogenic regions by the choroid plexus-CSF nexus. *J. Neural Transm (Vienna).* **118** (1), 115–133 (2011).
24. Novakova Martinkova, J. et al. Longitudinal progression of choroid plexus enlargement is associated with female sex, cognitive decline and ApoE E4 homozygote status. *Front. Psychiatry.* **14**, 1039239 (2023).
25. Čarna, M. et al. Pathogenesis of Alzheimer's disease: Involvement of the choroid plexus. *Alzheimer's Dement.* (2023).
26. Tadayon, E., Pascual-Leone, A., Press, D., Santarnecchi, E. & Initiative, A. D. N. Choroid plexus volume is associated with levels of CSF proteins: relevance for Alzheimer's and Parkinson's disease. *Neurobiol. Aging.* **89**, 108–117 (2020).
27. Choi, J. D. et al. Choroid plexus volume and permeability at brain MRI within the alzheimer disease clinical spectrum. *Radiology* **212400**. (2022).
28. Alisch, J. S. et al. Characterization of Age-Related differences in the human choroid plexus volume, microstructural integrity, and blood perfusion using multiparameter magnetic resonance imaging. *Front. Aging Neurosci.* 613. (2021).
29. Dyke, C. G. Indirect signs of brain tumor as noted in routine Roentgen examinations. Displacement of the pineal shadow. (A survey of 3000 consecutive skull examinations). *Am. J. Roentgenol.* **23**, 598–606 (1930).
30. Modic, M. et al. Calcification of the choroid plexus visualized by computed tomography. *Radiology* **135** (2), 369–372 (1980).
31. Wegiel, J. et al. Vascular fibrosis and calcification in the hippocampus in aging, alzheimer disease, and down syndrome. *Acta Neuropathol.* **103**, 333–343 (2002).
32. Nicolas, G., Charbonnier, C., Campion, D. & Veltman, J. A. Estimation of minimal disease prevalence from population genomic data: application to primary Familial brain calcification. *Am. J. Med. Genet. B Neuropsychiatr Genet.* **177** (1), 68–74 (2018).
33. De Leon, M. et al. The radiologic prediction of alzheimer disease: the atrophic hippocampal formation. *Am. J. Neuroradiol.* **14** (4), 897–906 (1993).
34. Jack, C. R. et al. Antemortem MRI findings correlate with hippocampal neuropathology in typical aging and dementia. *Neurology* **58** (5), 750–757 (2002).
35. Morris, J. C. et al. The uniform data set (UDS): clinical and cognitive variables and descriptive data from alzheimer disease centers. *Alzheimer Disease Assoc. Disorders.* **20** (4), 210–216 (2006).
36. Tahmi, M., Bou-Zeid, W. & Razlighi, Q. R. A fully automatic technique for precise localization and quantification of Amyloid- β PET scans. *J. Nucl. Med.* **60** (12), 1771–1779 (2019).
37. Mosconi, L. et al. Increased fibrillar amyloid- β burden in normal individuals with a family history of late-onset Alzheimer's. *Proc. Natl. Acad. Sci.* **107** (13), 5949–5954 (2010).
38. Zou, K. H. et al. Statistical validation of image segmentation quality based on a Spatial overlap index. *Acad. Radiol.* **11** (2), 178–189 (2004).
39. Kim, J. H. Multicollinearity and misleading statistical results. *Korean J. Anesthesiology.* **72** (6), 558–569 (2019).
40. Adams, L. C. et al. Diagnostic performance of susceptibility-weighted magnetic resonance imaging for the detection of calcifications: a systematic review and meta-analysis. *Sci. Rep.* **7** (1), 1–10 (2017).
41. Wehrli, F. W. Magnetic resonance of calcified tissues. *J. Magn. Reson.* **229**, 35–48 (2013).
42. Serot, J.-M., Béné, M.-C., Foliguet, B. & Faure, G. C. Morphological alterations of the choroid plexus in late-onset Alzheimer's disease. *Acta Neuropathol.* **99**, 105–108 (2000).
43. Yin, C. et al. ApoE attenuates unresolvable inflammation by complex formation with activated C1q. *Nat. Med.* **25** (3), 496–506 (2019).
44. Fujiyoshi, M., Ohtsuki, S., Hori, S., Tachikawa, M. & Terasaki, T. 24S-hydroxycholesterol induces cholesterol release from choroid plexus epithelial cells in an apical-and ApoE isoform-dependent manner concomitantly with the induction of ABCA1 and ABCG1 expression. *J. Neurochem.* **100** (4), 968–978 (2007).
45. Lotze, M. et al. Novel findings from 2,838 adult brains on sex differences in Gray matter brain volume. *Sci. Rep.* **9** (1), 1671 (2019).
46. van Eijk, L. et al. Region-specific sex differences in the hippocampus. *Neuroimage* **215**, 116781 (2020).
47. McEwen, B. Estrogen actions throughout the brain. *Recent Prog. Horm. Res.* **57**, 357–384 (2002).
48. Protopoulos, X. et al. Hippocampal structural changes across the menstrual cycle. *Hippocampus* **18** (10), 985–988 (2008).
49. Ferretti, M. T. et al. Sex differences in alzheimer disease — the gateway to precision medicine. *Nat. Reviews Neurol.* **14** (8), 457–469 (2018).
50. Meethal, S. V., Smith, M. A., Bowen, R. L. & Atwood, C. S. The gonadotropin connection in Alzheimer's disease. *Endocrine* **26**, 317–325 (2005).
51. Kass, R. E. & Raftery, A. E. Bayes factors. *J. Am. Stat. Assoc.* **90** (430), 773–795 (1995).

52. Kosaka, K. Diffuse neurofibrillary tangles with calcification: a new presenile dementia. *J. Neurol. Neurosurg. Psychiatry*. **57** (5), 594–596 (1994).
53. Tsolaki, E., Csincsik, L., Xue, J., Lengyel, I. & Bertazzo, S. Nuclear and cellular, micro and nano calcification in Alzheimer's disease patients and correlation to phosphorylated Tau. *Acta Biomater.* **143**, 138–144 (2022).
54. Wang, Y. et al. Clinical quantitative susceptibility mapping (QSM): biometal imaging and its emerging roles in patient care. *J. Magn. Reson. Imaging*. **46** (4), 951–971 (2017).
55. Rebeck, G. W. The role of APOE on lipid homeostasis and inflammation in normal brains: thematic review series: ApoE and lipid homeostasis in Alzheimer's disease. *J. Lipid Res.* **58** (8), 1493–1499 (2017).
56. Ossenkoppele, R. & Van der Flier, W. M. APOE genotype in the era of disease-modifying treatment with monoclonal antibodies against Amyloid-B. *JAMA Neurol.* **80** (12), 1269–1271 (2023).

Author contributions

Conceptualization: TAB. Methodology: IO, XW, YZ, SHH, TBSsoftware: IO, XW, YZ, SHH, QRR Validation: IO, XW, YZ, TAB Formal analysis: IO, XW, YZ, SHH, QRR, KX Investigation: IO, XW, YZ, KX, SHH, ET, TM, EKF, JPD, KC, SP, LBM, APC, WJD, QRR, LG, YL, GCC, HR, MJL, TAB Data curation: IO, XW, KX, SHH, ET, TM, EKF, JPD, MJL, TAB Writing - Original Draft: IO, TAB Writing - Review & Editing: IO, TAB Supervision: MJL, TAB All authors read and approved the final manuscript.

Funding

This work was supported by the National Institutes of Health [R56NS111052, R01 AG077576, R01AG072794 and R01AG078800-01] and Brain & Behavior Research Foundation NARSAD BBRF 223814-01.

Declarations

Competing interests

The authors declare no competing interests.

Ethical approval

This study was approved by the Institutional Review Boards of Weill Cornell Medicine and New York University.

Informed consent

Informed consent was obtained from all subjects and/or their legal guardian(s).

Additional information

Supplementary Information The online version contains supplementary material available at <https://doi.org/10.1038/s41598-025-97409-1>.

Correspondence and requests for materials should be addressed to I.O. or T.A.B.

Reprints and permissions information is available at www.nature.com/reprints.

Publisher's note Springer Nature remains neutral with regard to jurisdictional claims in published maps and institutional affiliations.

Open Access This article is licensed under a Creative Commons Attribution-NonCommercial-NoDerivatives 4.0 International License, which permits any non-commercial use, sharing, distribution and reproduction in any medium or format, as long as you give appropriate credit to the original author(s) and the source, provide a link to the Creative Commons licence, and indicate if you modified the licensed material. You do not have permission under this licence to share adapted material derived from this article or parts of it. The images or other third party material in this article are included in the article's Creative Commons licence, unless indicated otherwise in a credit line to the material. If material is not included in the article's Creative Commons licence and your intended use is not permitted by statutory regulation or exceeds the permitted use, you will need to obtain permission directly from the copyright holder. To view a copy of this licence, visit <http://creativecommons.org/licenses/by-nc-nd/4.0/>.

© The Author(s) 2025